Charge Compensation Dynamics in the Redox Processes of Polypyrrole−Modified Electrodes

ARTICLE *in* THE JOURNAL OF PHYSICAL CHEMISTRY · SEPTEMBER 1996

Impact Factor: 2.78 · DOI: 10.1021/jp9607780

4 AUTHORS, INCLUDING:

Gilberto Maia
Universidade Federal de Mato Grosso do Sul
38 PUBLICATIONS **558** CITATIONS
SEE PROFILE

Roberto M Torresi
University of São Paulo
191 PUBLICATIONS **3,734** CITATIONS
SEE PROFILE

Edson A. Ticianelli
University of São Paulo
192 PUBLICATIONS **6,225** CITATIONS
SEE PROFILE

Charge Compensation Dynamics in the Redox Processes of Polypyrrole-Modified Electrodes

Gilberto Maia,† Roberto M. Torresi,* Edson A. Ticianelli, and Francisco C. Nart

Instituto de Química de São Carlos, Universidade de São Paulo, 13564-970 São Carlos (SP), Brazil

Received: March 13, 1996; In Final Form: July 2, 1996[⊗]

Electrochemical quartz crystal microbalance (EQCM) data combined with cyclic voltammetry were used to study the ionic exchange process in polypyrrole films prepared in sulfuric acid solution. A quantitative analysis of the results indicates a doping degree of 33% after polymerization and a high polymerization efficiency. Studies performed in monomer-free solutions of Na_2SO_4, $NaNO_3$, and Cs_2SO_4 show that both anions and cations are involved in the charge compensation process. The analysis of the ionic exchange is made using the integral quantities (charge, mass, number of moles, and molar fraction) and differential quantities (ionic fluxes and transport number). The results of such quantitative calculations are interpreted taking also into account the transfer of neutral species like solvent molecules and the physicochemical nature of the anions and cations involved in the redox process.

Introduction

It has been shown that the electrochemical response and cycle stability of electroactive polymers such as polypyrrole (PPy) are dependent on the ionic transport necessary to maintain electroneutrality.[1−6] Therefore, the understanding of the nature of transport processes in electroactive polymers is necessary for developing useful materials for electrochemical devices.

Several analytical techniques, such as electrochemical and spectroelectrochemical methods,[7−9] electrochemical quartz crystal microbalance,[10,11] ellipsometry,[12,13] optical beam deflection,[14] scanning electrochemical microscopy,[15] Rutherford backscattering,[16,17] and luminescence probe,[18] have been used to study the charge compensation process in conducting polymers to obtain information about the relative contribution of the anions and cations to this phenomenon.

It is accepted that the role played by ions and solvent molecules exchanged across a polymer film differ greatly depending on the physicochemical nature of these ions and the way of the polymeric film was obtained. Naoi et al.,[19] for example, concluded that for PPy doped with ClO_4^- or BF_4^- the charge compensation is accomplished by anions during the oxidation process. In the case of PPy doped with polymeric anions like poly(styrenesulfonate) or poly(vinylsulfonate), the ejection of cations and solvent molecules has been reported.[19,20] On the other hand, when PPy films were obtained in the presence of surfactant anions like dodecylbenzenesulfonate, cations and anions are involved in the electroneutralization process.[14,21] Another way to manipulate the ionic transport process during the redox cycling of the conducting polymer has been achieved by using composite films like polyaniline/Nafion[22] or poly(styrenesulfonate)/poly(xylylviologen).[23]

This work describes a study of the formation of PPy films and ion transport during the redox reaction. The electrolyte was changed in order to investigate the influence of the chemical nature of the ions on the charge compensation process. The electrochemical quartz crystal microbalance (EQCM) is used to identify the ions which participate in the redox process and the contribution of cations and anions to charge-compensation motion during the injection/ejection of electrons in these films. We are proposing two new parameters calculated from mass change and current density: the molar fraction (x_i) and the transport number (t_i). These parameters give the ratio between anions and cations participating in the electroneutralization process. The analysis of both, x_i ant t_i as a function of potential shows that these quantities strongly depend on the chemical nature of ions taking part in the redox reaction. Thus, the mathematical approach proposed in this full paper allows to identify the role played by each individual species in the charge compensation process.

Experimental Section

PPY films were grown on a gold electrode by applying a constant current of 4 mA/cm^2 from an aqueous 58 mM pyrrole (Py) + 0.5 M sulfuric acid solution. After deposition, the films were rinsed with distilled water and placed in the electrochemical cell with deaerated monomer-free solutions of 0.5 M $NaNO_3$, 0.17 M Na_2SO_4, or 0.17 M Cs_2SO_4 as electrolytes. A platinum wire was used as counter electrode, and all potentials are referred to the saturated calomel electrode (SCE). Electrochemical measurements on PPy films were performed under potentiodynamic conditions. Variation of current was recorded simultaneously with the change of quartz resonance frequency as a function of potential.

The working electrode was an AT-cut 6 MHz quartz crystal (16 mm in diameter) with the gold layer deposited in key form on both sides (active area = 0.2 cm^2). This piezoelectric element was mounted in a Teflon holder, and one of the gold layer, in contact with the electrolytic solution, was attached to both the oscillator circuit and FAC 2.1 potentiostat and, thereby, to ground. The resonance frequency shift was measured with an HP 5671 Universal Counter, and the data were stored in a personal computer.

The mass of the deposited film was a linear function of the charge for all films studied. The thickness of the PPy film was small compared with the thickness of the crystal, and it behaves in a rigid manner. Thus, the Sauerbrey treatment $\Delta f = -K\Delta m$ can be used to relate the mass changes per unit area, Δm (in g/cm^2), with the resonance frequency shift, Δf (in Hz). A K value of 5.2×10^7 Hz g^{-1} cm^2 was used for this EQCM.[24]

Results and Discussion

Synthesis of Polypyrrole Films. Figure 1 shows the variation of potential and mass as a function of time during the galvanostatic polymerization of pyrrole in the presence of H_2SO_4. During the polymer synthesis a potential value of ca.

† Present address: Universidade Federal do Mato Grosso, Campo Grande, Brazil.

⊗ Abstract published in *Advance ACS Abstracts,* September 1, 1996.

S0022-3654(96)00778-2 CCC: $12.00

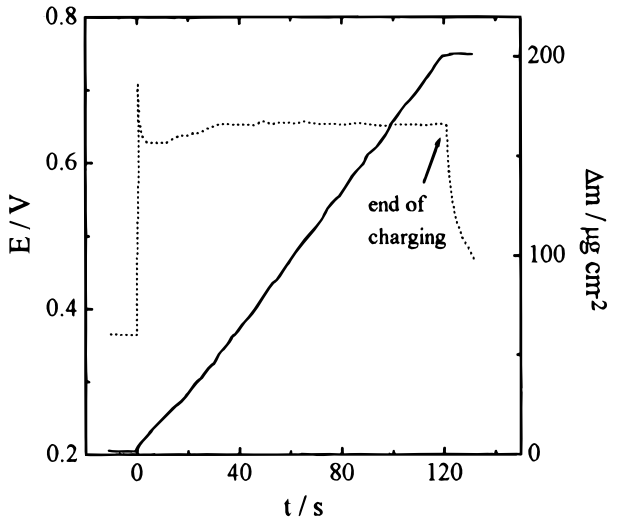

Figure 1. EQCM Δm (—) and potential (···) responses recorded during the galvanostatic deposition of PPy films. $j = 4$ mA cm^{-2}.

0.65 V was reached, and the mass increased linearly with time until the current supply was stopped. The mechanism proposed earlier for PPy electroformation takes into consideration not only the formation but also the oxidation of the film:[5,13,25−29]

$$[\mathrm{Py(HSO_4)_{0.33}}]_n + \mathrm{Py} + 0.33\mathrm{HSO_4^-} \rightarrow [\mathrm{Py(HSO_4)_{0.33}}]_{n+1} + 2\mathrm{H^+} + 2.33\mathrm{e^-} \quad (1)$$

This mechanism considers that a charge equivalent to 2.33 electrons per molecule will lead to the addition of one molecule of pyrrole and 0.33 molecules of the doping anion (HSO_4^-).[13,19,20] Consequently, according to reaction 1, the electropolymerization charge, q_p, can be written as

$$q_p = 2.33nF \quad (2)$$

where n is the number of Py moles added and F is the Faraday constant.

From reaction 1, the total mass gain during the PPy film growth can be written as

$$\Delta m = n\sum_i \mathrm{MW}_i = n(\mathrm{MW_{Py}} + 0.33\mathrm{MW_{HSO_4^-}} - 2\mathrm{MW_{H^+}}) \quad (3)$$

where MW_{Py} is the molar mass of pyrrole, $MW_{HSO_4^-}$ is the molar mass of bisulfate, and MW_{H^+} is the molar mass of proton. By dividing eq 3 by eq 2 and substituting the values of the molar masses, the mass/charge relationship is obtained as follows:

$$\left(\frac{\Delta m}{q}\right)_{\mathrm{theor}} = \frac{\mathrm{MW_{Py}} + 0.33\mathrm{MW_{HSO_4^-}} - 2\mathrm{MW_{H^+}}}{2.33F} = 0.43\,\frac{\mathrm{mg}}{\mathrm{C}} \quad (4)$$

This value was calculated disregarding solvent participation. On the hypothesis that the film formed has incorporated water molecules during the electropolymerization process, the experimental value should be greater than 0.43 mg/C. However, a value of 0.40 mg/C (Figure 1) was obtained experimentally, showing a high polymerization efficiency and that the film formed is poorly hydrated. This fact also indicates that, in strong acid media, the parallel reaction corresponding to an oxidative chain stopping reaction

$$\mathrm{PPy} + \mathrm{H_2O} \rightarrow \mathrm{PPy - (OH)} + 2\mathrm{H^+} + 2\mathrm{e^-} \quad (5)$$

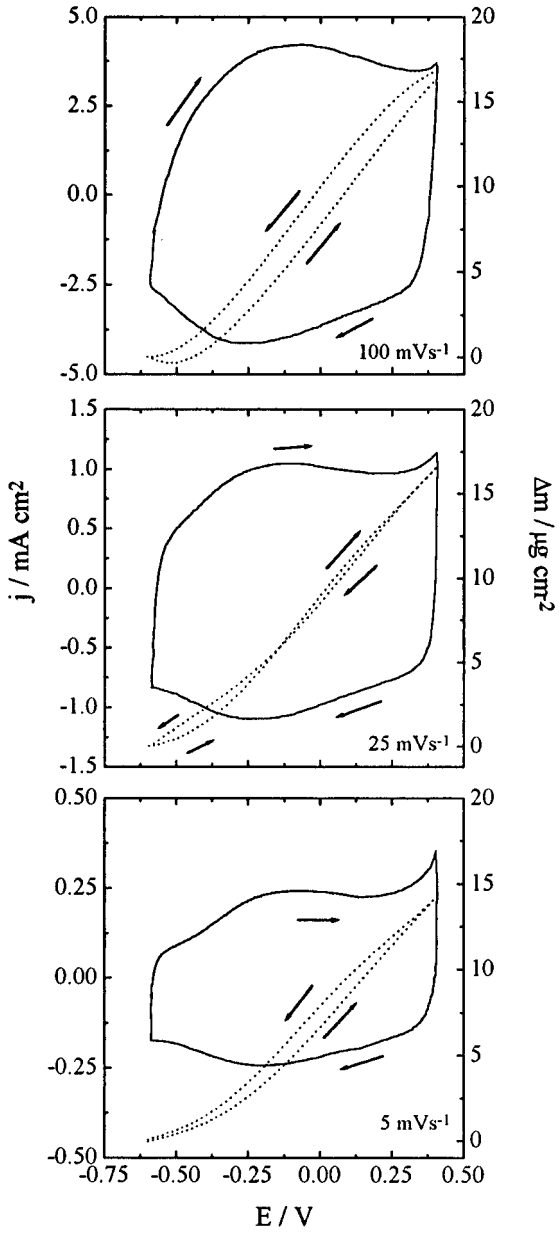

Figure 2. Potentiodynamic j/E (—) and $\Delta m/E$ (···) profiles for 0.5 M $NaNO_3$ electrolytic solution for different scan rates.

does not take place in a significative manner as it was observed in syntheses carried out in neutral media.[13]

Charge Compensation Dynamics in Monomer-Free Solutions. *Experimental Results.* Figure 2 shows the stationary j/E and $\Delta m/E$ potentiodynamic profiles recorded for different sweep rates in the $NaNO_3$ electrolyte. It can be seen that in all cases the oxidation process is accompanied by a mass increase, showing that the electroneutralization of the film is achieved mainly by the participation of nitrate anions. It has to be pointed out that, in the range of sweep rates studied, no large differences neither in the voltammogram nor in the mass profiles are observed.

Figure 3 shows the stationary j/E and $\Delta m/E$ potentiodynamic profiles recorded for different sweep rates in the Na_2SO_4 electrolyte. By comparing with the results in Figure 2, the most striking feature to be noted is the dependence not only of the voltammogram but also of the mass profile on the sweep rate. On the other hand, it is also seen that both j/E and $\Delta m/E$ profiles depend on the chemical nature of the anion. While in nitrate solutions the charge compensation is made mainly by the accommodation of anions, in sulfate electrolyte, the charge compensation is achieved by the participation of both positive

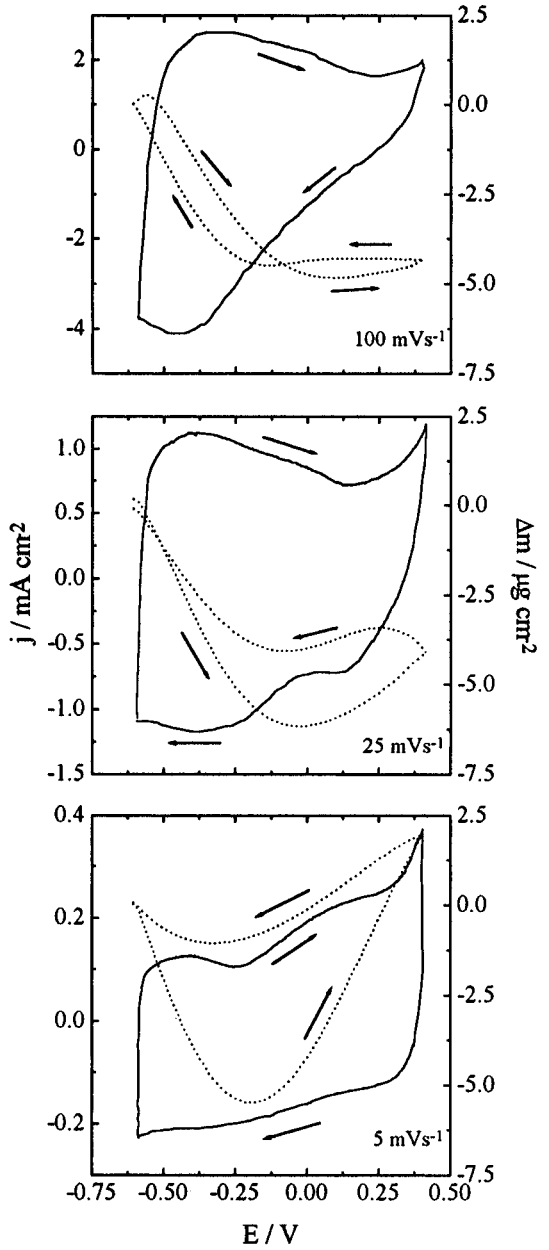

Figure 3. Potentiodynamic j/E (—) and $\Delta m/E$ (···) profiles for 0.17 M Na_2SO_4 electrolytic solution for different scan rates.

and negative ions. In the last case, in the beginning of the oxidation process, a fast diminution of mass is observed, showing that the ejection of cation is predominant. Above ca. −0.1 V, a dependence of the mass behavior on the sweep rate is observed, showing that the lower is the sweep rate, the higher is the incorporation of sulfate anions. Another fact to point out in Figure 3 is that the hysteresis between anodic and cathodic waves of mass profiles increases when the sweep rate diminishes. At 5 mV/s the charge compensation is reached in a completely different way in both waves. The appearance of two current maxima in the voltammograms at the lower sweep rate can be associated with the fact that the rate of injection/ejection of the ions occurs not simultaneously but in sequence, stressing their dependence with the electrode potential.

In order to study the influence of cations, experiments in Cs_2SO_4 were carried out. Figure 4 shows the stationary j/E and $\Delta m/E$ potentiodynamic profiles recorded for different sweep rates in the Cs_2SO_4 electrolyte. In this case, it is observed that the form of the voltammogram is approximately the same, independent of the sweep rate. On the other hand, in all cases, a mass diminution during the oxidation process with the corresponding increase for reduction is observed. These results

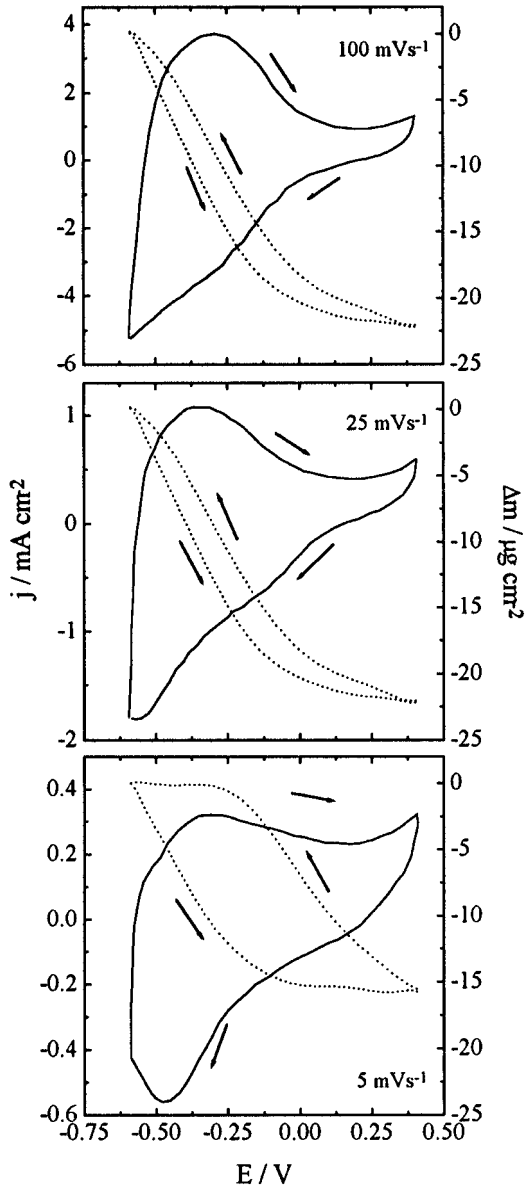

Figure 4. Potentiodynamic j/E (—) and $\Delta m/E$ (···) profiles for 0.17 M Cs_2SO_4 electrolytic solution for different scan rates.

lead to the conclusion that the charge compensation process is mainly made by the ejection/insertion of cesium cations. It has to be noted that the hyteresis of mass profile increases when the sweep rate diminishes.

In order to compare the dynamics of ions exchange during the redox process in the several electrolytes for 5 and 100 mV/s, EQCM data were compared by plotting Δm versus charge density, as shown in Figure 5. In the same way as in the potentiodynamic profiles, it can be inferred that the behavior depends of the chemical nature of the electrolyte and on the sweep rate. Normally this kind of analysis is made to identify the ions involved in the charge compensation process, but in the cases treated here, there are only two situations where this identification is possible. In Na_2SO_4 electrolyte at 5 mV/s there is a linear relationship of the Δm vs q plot at low anodic charge with a value of the slope of 0.84 mg/C. With this slope and considering that the charge compensation is made only by cation releasing, it is possible to calculate the number of water molecules linked to the sodium cation using eqs 6−8 without anions contribution. The value obtained from such calculation is 3. The same calculation made for Cs_2SO_4 electrolyte shows that in the beginning of the oxidation process the charge compensation is made by the release of cesium cations without water molecules bonded to it.

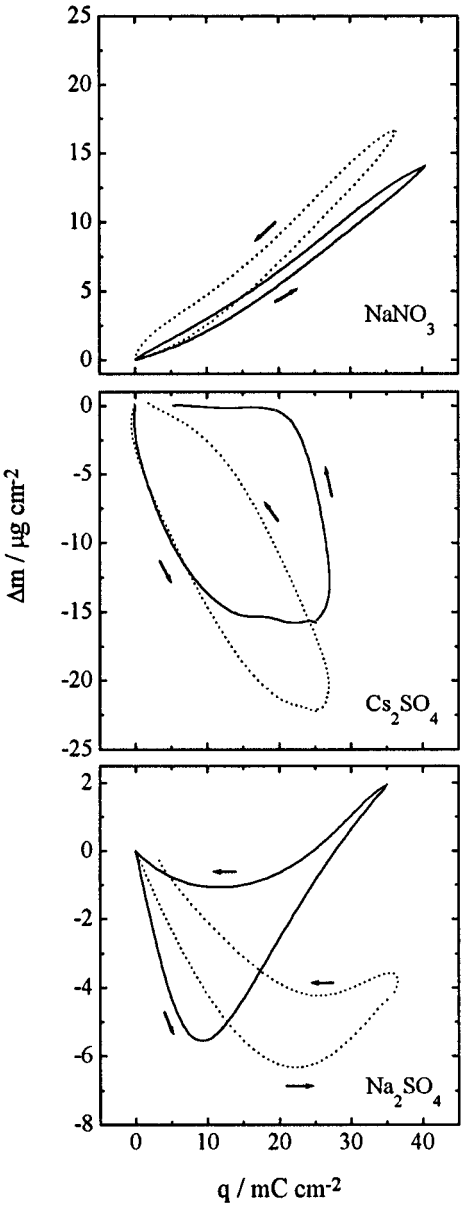

Figure 5. Mass change (Δm) as function of charge density for PPy film in different electrolytic solutions: (—) 5 and (···) 100 mV/s.

Data Processing. Considering the participation of positive and negative ions, at the limiting polymer/solution boundary, the mass change can be written as

$$\Delta m = \sum_i MW_i \xi_i + \sum_n MW_n \xi_n = MW_c \xi_c + MW_a \xi_a + MW_{H_2O} \xi_{H_2O} \quad (6)$$

where MW_i is the molar mass of the ionic species and MW_n is the molar mass of neutral species. The ξ quantity corresponds to the amount of moles exchanged, which is a function of the charge passed through the electrode/polymer interface. In this work, the second part of eq 6 represents the exchange of cation (c), anion (a), and solvent molecule (H_2O), where the moles of solvent molecules could be associated with the hydration layer (h) of the cations, and it can be rewritten as

$$\xi_{H_2O} = h\xi_c \quad (7)$$

The electric charge passed through the electrode/polymer interface is given by

$$q = -\sum_i z_i F \xi_i = -z_c F \xi_c - z_a F \xi_a \quad (8)$$

where $z_i F$ is the charge carried per mole of species i.

Combining eqs 6−8 and considering $z_c = 1$, an expression to calculate the number of moles exchanged in the redox process as a function of potential is obtained:

$$\xi_{c(E)} = \frac{\Delta m_{(E)}}{\left(MW_c + \frac{MW_a}{|z_a|} + hMW_{H_2O}\right)} - \frac{MW_a q_{(E)}}{|z_a| F \left(MW_c + \frac{MW_a}{|z_a|} + hMW_{H_2O}\right)} \quad (9)$$

$$\xi_{a(E)} = \frac{\Delta m_{(E)}}{(|z_a| MW_c + MW_a + |z_a| hMW_{H_2O})} + \frac{(MW_c + hMW_{H_2O}) q_{(E)}}{F(|z_a| MW_c + MW_a + |z_a| hMW_{H_2O})} \quad (10)$$

Following the results of these equations, the amounts of cations and anions exchanged during redox process for two different sweep rates in Na_2SO_4 solution were calculated, and they are shown in Figure 6. The same calculation was also made for the other experimental conditions. These results were used to obtain the molar fraction (x_i) of the ions given by

$$x_i = \xi_i / \sum_i \xi_i \quad (11)$$

Figure 7 shows the x_i/E profiles for the cations at different sweep rates for all electrolytes used here. The negative values of x_i are referred to the ejection of cations from the film.

In order to compare the above results obtained in terms of the integral quantities q, Δm, and ξ, the net instantaneous molar flux of species i ($d\xi_i/dt$ in mol cm^{-2} s^{-1}) within the film was calculated by differentiating eqs 9 and 10:

$$\frac{d\xi_{c(E)}}{dt} = \frac{d(\Delta m_{(E)})}{dt} \frac{1}{\left(MW_c + \frac{MW_a}{|z_a|} + hMW_{H_2O}\right)} - \frac{MW_a j_{(E)}}{|z_a| F \left(MW_c + \frac{MW_a}{|z_a|} + hMW_{H_2O}\right)} \quad (12)$$

and

$$\frac{d\xi_{a(E)}}{dt} = \frac{d(\Delta m_{(E)})}{dt} \frac{1}{(|z_a| MW_c + MW_a + |z_a| hMW_{H_2O})} + \frac{(MW_c + hMW_{H_2O}) j_{(E)}}{F(|z_a| MW_c + MW_a + |z_a| hMW_{H_2O})} \quad (13)$$

The flux was considered positive when species are inserted to polymer film and negative in the case of they are ejected. Figures 8 and 9 show the plots of these differential quantities as a function of potential for $NaNO_3$ and Na_2SO_4 electrolytes. These results were used to calculate the transport number which provides a better understanding of the participation of the cations and anions in the redox process.

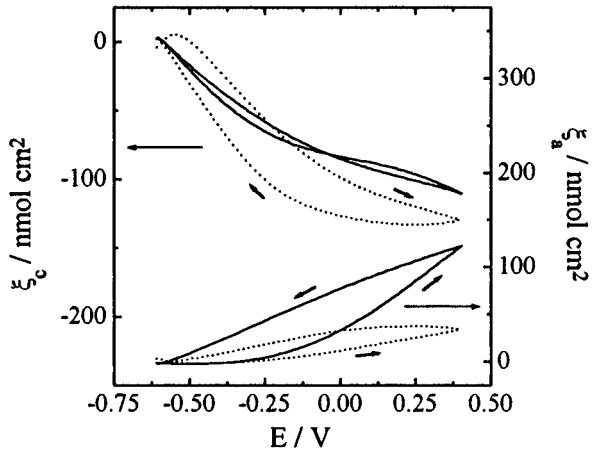

Figure 6. Moles of ionic species exchanged as a function of potential for 0.17 M Na_2SO_4 electrolytic solution: (—) 5 and (···) 100 mV/s.

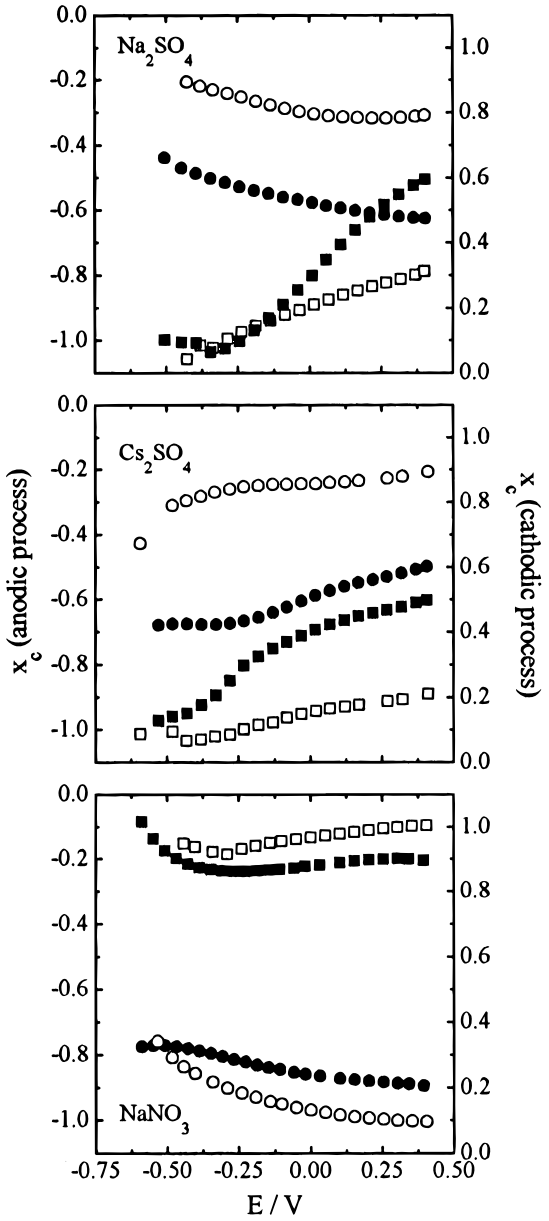

Figure 7. Mole fraction of cations as a function of potential for the different electrolytic solutions. Anodic sweep: (■) 5 and (□) 100 mV/s. Cathodic sweep: (●) 5 and (○) 100 mV/s.

Figure 10 shows the transport number of cationic species (t_c) for all electrolytes used in this work. Negative values of t_c were referred to ejected cations from the film.

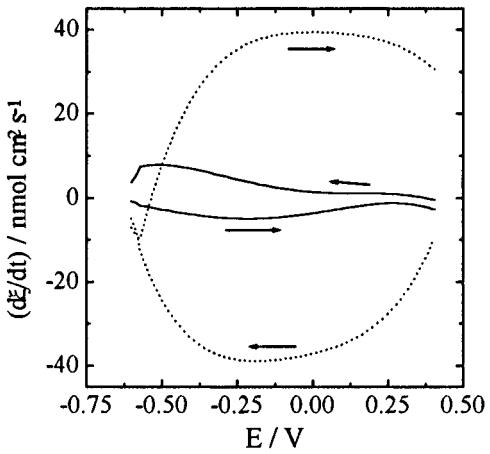

Figure 8. Instantaneous ionic fluxes as a function of potential for 0.5 M $NaNO_3$ electrolytic solution: (—) cations and (···) anions. $\upsilon = 100$ mV/s.

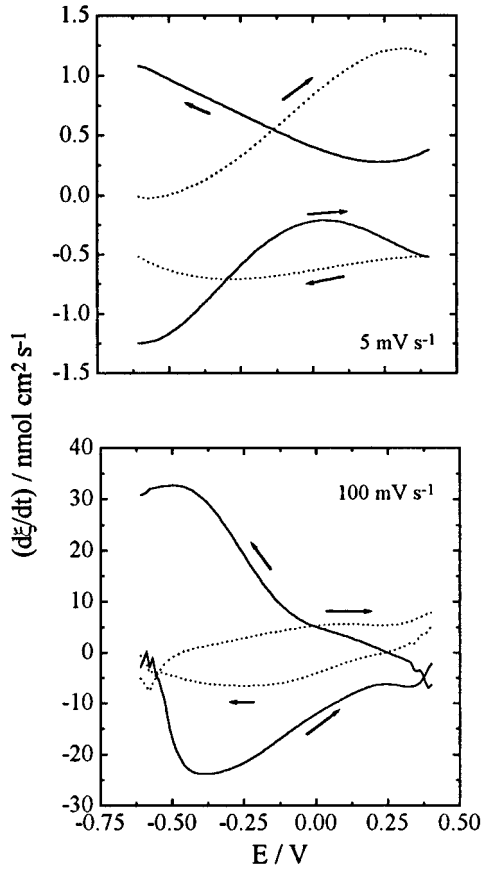

Figure 9. Instantaneous ionic fluxes as a function of potential for 0.17 M Na_2SO_4 electrolytic solution for two different sweep rates: (—) cations and (···) anions.

$$t_i = \frac{F(\mathrm{d}\xi_i/\mathrm{d}t)}{j} = \frac{\mathrm{d}\xi_i/\mathrm{d}t}{\sum_i |z_i||\mathrm{d}\xi_i/\mathrm{d}t|} \qquad (14)$$

Data Analysis. From Figure 6, it is seen that there is a strong dependence of the ξ/E profiles with the sweep rate, the anionic exchange being higher when the sweep rate is smaller. However, this behavior is strongly dependent on the chemical nature of the electrolyte, and a more detailed analysis can be made using the molar fractions as defined in eq 11 (see Figure 7). These results show that in nitrate solution there is no deep influence of the sweep rate on the x_c/E profiles; on the contrary, this is not the case for sulfate solutions, where the participation of cations is more important at high sweep rates showing that

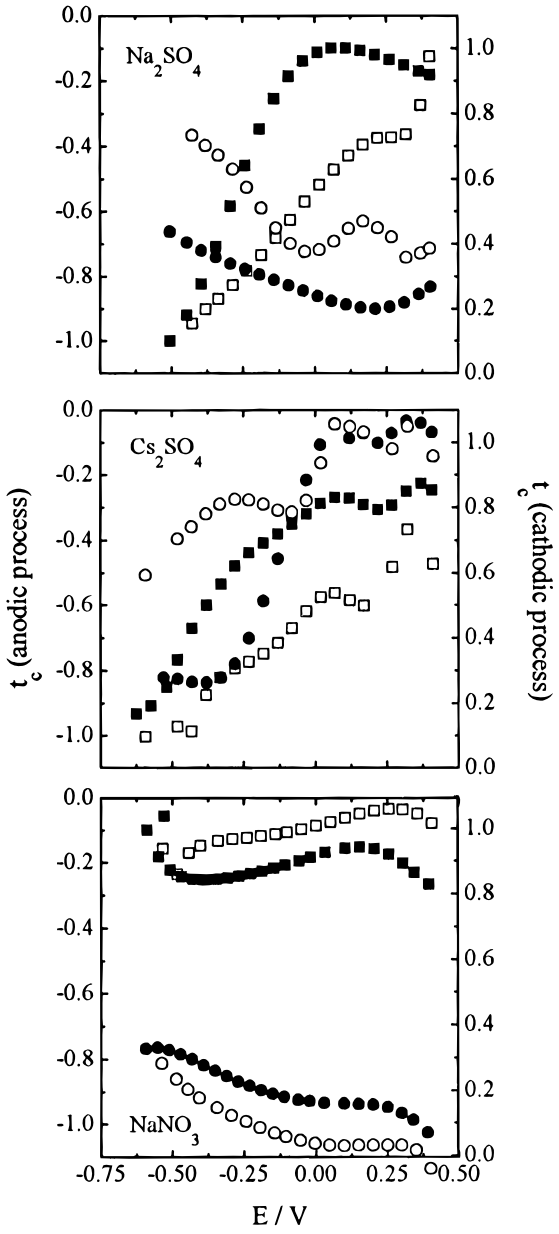

Figure 10. Transport number of cations as a function of potential for the different electrolytic solution. Anodic sweep: (■) 5 and (□) 100 mV/s. Cathodic sweep: (●) 5 and (○) 100 mV/s.

the movement of sulfate is important only when the potential is sweeped very slowly. In these electrolytes, in the anodic sweep, x_c is equal to 1 until ca. −0.25 V, independent of the scan rate; i.e., anion incorporation only starts at this potential.

From the results obtained in Na^+ solutions (Figure 7), it is possible to conclude that the nature of the anion is very important for the charge compensation process. In the whole potential range, $x_{NO_3^-} > x_{SO_4^{2-}}$, meaning that an anion with smaller charge/size relationship can be more easily incorporated into the PPy matrix. On the other hand, in the sulfate electrolytes, there are some differences between the behavior of the cations specially in the cathodic sweep. In both cases, there is exchange of anions and cations, but the behavior as a function of potential changes with the nature of the electrolyte. The Na^+ ions increase their participation while Cs^+ ions slightly diminish when the potential becomes more negative.

An analysis of the ionic flux is important because these quantities are independent of the redox reaction kinetics. In the case of nitrate solution (Figure 8), the flux of injected (anodic process) or ejected (cathodic process) anions is higher than the corresponding flux of cations, both depending slightly on the sweep rate. For Na_2SO_4 solution (Figure 9), the ionic flux strongly depends on the sweep rate. In the anodic sweep at 5 mV/s, the flux of incorporated anions increases from −0.5 V to more positive potentials being higher than the flux of ejected cations above −0.25 V. When the potential sweep is reversed, the anionic flux is approximately constant, while the cationic flux increases with the potential. However, in the anodic sweep at 100 mV/s, the flux of ejected cations defines a maximum at around −0.375 V, and it is more important than the flux of anions practically in all potential range. When the potential sweep is reversed, the flux of injected cations also present a maximum at −0.5 V. It is seen that the anodic and the cathodic cations flux profiles are similar to those of the cyclic voltammograms, and this fact puts in evidence that in these experimental conditions the polymer film electroneutrality is mainly achieved by ejection/injection of cations. Although not shown in a figure, it was seen that the flux profiles in Cs_2SO_4 solution at 100 mV/s are similar to those on Na_2SO_4. Besides that, also at 5 mV/s, the cationic and anionic fluxes define a maximum in accordance with the j/E profile.

The transport number allows to identify the charge contribution of the species responsible for achieving the electroneutrality of the PPy film. This quantity is not affected by the kinetic characteristics, and with the change in electrolyte it is possible to analyze the redox behavior of the PPy film with respect to the ionic chemical nature (Figure 10). In the case of the sulfate solutions, there is a diminution of t_c with the potential in the oxidation process. At 5 mV/s for potentials higher than 0.1 V, $t_{Cs^+} \approx 0.3$ and $t_{Na^+} \approx 0.1$, showing that cesium cations are expelled from the polymer easier than sodium cations. An explanation to this can be found on the basis of the Lewis acid strength of the cations. A measure of the Lewis acid strength is obtained from an empirical relationship,[30,31] and it depends on the charge number of the atomic nucleus, the empirical ionic radius of the element, and the electronegativity of the element in the corresponding oxidation state. The Lewis acid strengths for cesium and sodium cations are 1.483 and 1.382, respectively.[31] In the oxidation process, positive charges are created in the polymer chain. A more acid donor element such as Cs^+ will be repulsed strongly by another positive charge, leading to a higher transport number in the anodic process at more positive potentials. In the beginning of the reduction process the difference between the two cations is more pronounced ($t_{Cs^+} \approx 1$ and $t_{Na^+} \approx 0.2$). In this case, positive charges are neutralized in the PPy chain network, and the uncompensated negative charge inside the matrix will act with a strong electrostatic force on a more acid donor element like Cs^+, leading to a higher participation in the charge compensation process.

It can also be seen that the transport number of sulfate ion depends on the sweep rate. At high sweep rate $t_{SO_4^{2-}}$ is small. This fact can be explained taking into account that the two negative charges of sulfate make the mobility of this anion more difficult in the polymer matrix because it is attached to two positive centers in the matrix. That is to say, that to inject/eject sulfate anions two positive charges must appear or disappear simultaneously or an ion pair such as $CsSO_4^-$ or $NaSO_4^-$ must be moved.

For Na^+ solution, in all cases the participation of the nitrate anions is more important than that of sulfate. This behavior agrees well with the results obtained in sulfate solutions at different sweep rates, showing that the incorporation/expulsion of anions with one negative charge is easier than anions with higher oxidation state.

A summary of the evidence for the identification of the species involved in the doping/undoping process is as follows:

Using the $\Delta m/q$ profiles, it was found that both cations and anions participate in the charge compensation, but in the beginning of the oxidation process in sulfate solution only the cation is expelled from the polymer matrix. By this way, it was possible to calculate the quantity of solvent molecules attached to the sodium and cesium cations. The hysteresis in these plots shows that the exchange of ions depends if positive charges are injected in the polymer (oxidation process) or if negative charges are created (cathodic process).

The introduction of the quantity ξ and x as a function of potential allowed to identify the relative amount of species involved, and this was found to be dependent on the chemical nature of the ions. However, since these integral quantities could be affected by kinetic problems, a further insight could be obtained with the differential quantities, that is, the fluxes of ions and the transport numbers. Regarding the last property, the following points could be stressed: First, at the faster scan rate (100 mV/s), smaller values of $t_{SO_4^{2-}}$ are observed, and this is related to the fact that this anion is attached to two positive charges. Second, the participation of the cations depends on their Lewis acid strength, which determines the electrostatic interaction between the cations and the electric charge in the polymer matrix. Third, the differences observed between nitrate and sulfate can also be explained in terms of their charge/size relationship.

Conclusions

This work has demonstrated that with the EQCM it is possible to calculate the percentage of dopant in PPy. Comparing the theoretical and experimental mass/charge value for the polymerization reaction, it is possible to have a notion about the polymerization efficiency.

It was also demonstrated that the participation of the ions in the electroneutralization process changes with the chemical nature of these ions. Finally, this work indicated that the calculation of transport number is a good strategy to evaluate the contribution of the different ions to the transport process which occurs simultaneously with the injection into or ejection of electrons in PPy thin films.

Acknowledgment. R.M.T. is grateful to FAPESP (Grant 94/2525-0) for the support of this work, and G.M. is grateful to CNPq for the PhD scholarship.

References and Notes

(1) Orata, D.; Buttry, D. A. *J. Am. Chem. Soc.* **1987,** *109*, 3574−3581.
(2) Córdoba-Torresi, S.; Gabrielli, C.; Keddam, M.; Takenouti, H.; Torresi, R. *J. Electroanal. Chem.* **1990,** *290*, 269−274.
(3) Hillman, A. R.; Swann, M. J.; Bruckenstein, S. *J. Phys. Chem.* **1991,** *95*, 3271−3277.
(4) Bácskai, J.; Kertész, V.; Inzelt, G. *Electrochim. Acta* **1993,** *38*, 393−397.
(5) Peres, R. C. D.; De Paoli, M. A.; Torresi, R. M. *Synth. Met.* **1992,** *48*, 259−270.
(6) Torresi, R. M.; Córdoba de Torresi, S. I.; Gabrielli, C.; Keddam, M.; Takenouti, H. *Synth. Met.* **1993,** *61*, 291−296.
(7) Lapkowski, M.; Geniès, E. M. *J. Electroanal. Chem.* **1990,** *279*, 157−168.
(8) Inzelt, G. In *Electroanalytical Chemistry;* Bard, A. J., Ed.; Marcel Dekker: New York, 1994; Vol. 18.
(9) Maia, G.; Ticianelli, E. A.; Nart, F. C. *Z. Phys. Chem.* **1994,** *186*, 245−257.
(10) Buttry, D. A. In *Electroanalytical Chemistry. A Series of Advances;* Bard, A. J., Ed.; Mardel Dekker: New York, 1991; Vol. 17, pp 1−85.
(11) Buttry, D. A.; Ward, M. D. *Chem. Rev.* **1992,** *92*, 1355−1379.
(12) Lee, C.; Kwak, J.; Bard, A. J. *J. Electrochem. Soc.* **1989,** *136*, 3720−3724.
(13) Sabatini, E.; Ticianelli, E. A.; Redondo, A.; Rubinstein, I.; Rishpon, J.; Gottesfeld, S. *Synth. Met.* **1993,** *55*−*57*, 1293−1298.
(14) Matencio, T.; De Paoli, M. A.; Peres, R. C. D.; Torresi, R. M.; Córdoba de Torresi, S. I. *Synth. Met.* **1995,** *72*, 59−64.
(15) Arca, M.; Mirkin, M. V.; Bard, A. J. *J. Phys. Chem.* **1995,** *99*, 5040−5050.
(16) Wainright, J. S.; Zorman, C. A. *J. Electrochem. Soc.* **1995,** *142*, 379−383.
(17) Wainright, J. S.; Zorman, C. A. *J. Electrochem. Soc.* **1995,** *142*, 384−388.
(18) Krishna, V.; Ho, Y. H.; Rajeshwar, K. *J. Am. Chem. Soc.* **1991**, *113*, 3325−3333.
(19) Naoi, K.; Lien, M.; Smyrl, W. H. *J. Electrochem. Soc.* **1991,** *138*, 440−445.
(20) Baker, C. K.; Reynolds, J. R. *J. Electroanal. Chem.* **1988,** *251*, 307−322.
(21) Torresi, R. M.; Córdoba de Torresi, S. I.; Matencio, T.; De Paoli, M. A. *Synth. Met.* **1995,** *72*, 283−287.
(22) Orata, D.; Buttry, D. A. *J. Electroanal. Chem.* **1988,** *257*, 71−82.
(23) Ostrom, G. S.; Buttry, D. A. *J. Phys. Chem.* **1995,** *99*, 15236−15240.
(24) Gabrielli, C.; Keddam, M.; Torresi, R. *J. Electrochem. Soc.* **1991,** *138*, 2657−2660.
(25) Scharifker, B. R.; Fermín, D. J. *J. Electroanal. Chem.* **1994,** *365*, 35−39.
(26) Pei, Q.; Qian, R. *Electrochim. Acta* **1992,** *37*, 1075−1081.
(27) Zhong, C.; Doblhofer, K. *Electrochim. Acta* **1990,** *35*, 1971−1976.
(28) Baker, C. K.; Qiu, Y. J.; Reynolds, J. R. *J. Phys. Chem.* **1991,** *95*, 4446−4452.
(29) Lien, M.; Smyrl, W. H.; Morita, M. *J. Electroanal. Chem.* **1991,** *309*, 333−340.
(30) Zhang, Y. *Inorg. Chem.* **1982,** *21*, 3886−3889.
(31) Zhang, Y. *Inorg. Chem.* **1982,** *21*, 3889−3893.

JP9607780